



Article scientifique

Article

2023

Published version

Open Access

This is the published version of the publication, made available in accordance with the publisher's policy.

Bioelectrocatalytic CO₂ Reduction by Mo-Dependent Formylmethanofuran Dehydrogenase

Sahin, Selmihan; Lemaire, Olivier N.; Belhamri, Mélissa; Kurth, Julia M.; Welte, Cornelia U.;
Wagner, Tristan; Milton, Ross Dean

How to cite

SAHIN, Selmihan et al. Bioelectrocatalytic CO₂ Reduction by Mo-Dependent Formylmethanofuran Dehydrogenase. In: Angewandte Chemie, 2023, vol. 62, n° 45, p. e202311981. doi: 10.1002/anie.202311981

This publication URL: <https://archive-ouverte.unige.ch/unige:173462>

Publication DOI: [10.1002/anie.202311981](https://doi.org/10.1002/anie.202311981)



Bioelectrocatalytic CO₂ Reduction by Mo-Dependent Formylmethanofuran Dehydrogenase

Selmihan Sahin⁺, Olivier N. Lemaire⁺, Mélissa Belhamri, Julia M. Kurth, Cornelia U. Welte, Tristan Wagner,* and Ross D. Milton*

Abstract: Massive efforts are invested in developing innovative CO₂-sequestration strategies to counter climate change and transform CO₂ into higher-value products. CO₂-capture by reduction is a chemical challenge, and attention is turned toward biological systems that selectively and efficiently catalyse this reaction under mild conditions and in aqueous solvents. While a few reports have evaluated the effectiveness of isolated bacterial formate dehydrogenases as catalysts for the reversible electrochemical reduction of CO₂, it is imperative to explore other enzymes among the natural reservoir of potential models that might exhibit higher turnover rates or preferential directionality for the reductive reaction. Here, we present electroenzymatic catalysis of formylmethanofuran dehydrogenase, a CO₂-reducing-and-fixing biomachinery isolated from a thermophilic methanogen, which was deposited on a graphite rod electrode to enable direct electron transfer for electroenzymatic CO₂ reduction. The gas is reduced with a high Faradaic efficiency (109 ± 1 %), where a low affinity for formate prevents its electrochemical reoxidation and favours formate accumulation. These properties make the enzyme an excellent tool for electroenzymatic CO₂-fixation and inspiration for protein engineering that would be beneficial for biotechnological purposes to convert the greenhouse gas into stable formate that can subsequently be safely stored, transported, and used for power generation without energy loss.

Our modern society currently faces the consequences of the increase in atmospheric carbon dioxide (CO₂) of the last century. Therefore, developing planet-scale CO₂-sequestration strategies and alternatives to fossil fuels for energy production has become an urgent matter. The reduction of

CO₂ constitutes an attractive solution to both problems^[1,2] but faces a challenge due to the high kinetic stability of CO₂. Chemical CO₂ reduction is often achieved using rare and polluting metals, as well as extreme operating conditions, to reach significant turnovers. Electrochemical CO₂ reduction could, in theory, provide attractive operating conditions, although high overpotentials are often required (making it energetically inefficient), and metallic electrocatalysts often lack selectivity.^[3–6] On the other hand, biological catalysts such as formate dehydrogenases (FDH) are great alternatives to perform CO₂-reduction as they operate under mild temperature, low pressure and with relatively low overpotential compared to electrochemical CO₂ reduction. Most enzymes have high selectivity, efficiency and exhibit turnover rates unmatched by most inorganic methods. The reaction product, formate, is stable, convenient for transport and a precursor for chemical production, energy generation, or to produce H₂,^[7] making formate an excellent surrogate to H₂ for renewable energy storage.^[8,9] Yet, FDHs were shown to be limited to relatively low turnover rates, substrate inhibition and relative instability, which is coherent with their physiological function of formate oxidation rather than CO₂ reduction, with rare exceptions.^[10]

Hydrogenotrophic methanogens are strict anaerobic microorganisms generating methane from the reduction of CO₂, a metabolism proposed to be among the first to appear on Earth.^[11,12] Their impressive short division period under chemolithotrophic conditions suggests that CO₂ reduction at high rates allows sufficient cellular energy acquisition. The entry point of carbon/energy acquisition is a functional equivalent to the FDH: the formyl-methanofuran (formyl-MFR) dehydrogenase (labelled Fwd or Fmd for the W- and

[*] S. Sahin, R. D. Milton
 University of Geneva, Department of Inorganic and Analytical Chemistry, Sciences II, Quai Ernest-Ansermet 30, 1211 Geneva 4 (Switzerland)
 E-mail: ross.milton@unige.ch

S. Sahin⁺
 Department of Chemistry, Faculty of Arts and Sciences, Suleyman Demirel University, Cunur, 32260 Isparta (Turkiye)

O. N. Lemaire, M. Belhamri, T. Wagner
 Max Planck Institute for Marine Microbiology, Celsiusstraße 1, 28359 Bremen (Germany)
 E-mail: twagner@mpi-bremen.de

J. M. Kurth, C. U. Welte
 Department of Microbiology, Institute for Water and Wetland Research, Radboud University, Heyendaalseweg 135, 6525 AJ Nijmegen (Netherlands)

J. M. Kurth
 Microcosm Earth Center - Philipps-Universität Marburg & Max Planck Institute for Terrestrial Microbiology, Hans-Meerwein-Str. 4, 35032 Marburg (Germany)

[†] These authors contributed equally to this work.

© 2023 The Authors. Angewandte Chemie International Edition published by Wiley-VCH GmbH. This is an open access article under the terms of the Creative Commons Attribution License, which permits use, distribution and reproduction in any medium, provided the original work is properly cited.

Mo-dependent isoforms, respectively, Figure 1A).^[13] Compared to FDHs, Fwd/Fmd is an all-in-one machinery capable of reversible CO₂ reduction and fixation following a two-step mechanism. In the first step, the subunits B and D, harbouring the same cofactor as FDH (a W/Mo-containing bis-pyranopterin guanosine dinucleotide, bis-PGD cofactor), perform CO₂ reduction to formate. The second step is the condensation of formate with the coenzyme MFR in subunit A catalysed by a [ZnZn] metallo-centre generating formyl-MFR and fuelling methanogenic metabolism. Structural studies suggested the sequestration of the formate in an internal cavity connecting the subunits B/D and A, facilitating the endergonic second reaction (Figure 1A). The electrons necessary for CO₂ reduction are derived from ferredoxin oxidation or direct electron transfers.^[13,14] Electrons transit through extensive FeS cluster relays made of polyferredoxin subunits. The abundance of [4Fe-4S] clusters may well be advantageous for heterogeneous electron transfer in bioelectrochemical systems (Figure 1).^[13-15] However, electrochemistry studies have not yet been assessed, likely due to the difficulty of growing Fwd/Fmd-producing organisms and the purification of these O₂-sensitive enzymes. Here, we describe a CO₂-reducing bioelectrocatalytic system using the Mo-dependent Fmd complex from a thermophilic methanogen, adsorbed onto a graphite rod electrode (GRE). The Fmd complex represents an opening play-

ground for electrochemical CO₂-fixation strategies as it does not require any mediator or covalent surface modification and exhibits direct electron transfer (DET)-type bioelectrocatalysis with the appreciable property of electrocatalyzing CO₂ reduction by two orders of magnitude greater than formate oxidation.

The native formyl-MFR complex from the thermophilic methanogen *Methanococcus shengliensis* was purified anaerobically by multistep chromatography (Figure S1A). Induced coupled plasma mass spectrometry (ICP-MS) demonstrated the presence of 0.9 mol of molybdenum per mol of the purified monomeric enzyme, which is therefore referred to as the Mo-dependent MsFmd complex. The complex appears to be made of five subunits by denaturing SDS-PAGE analysis, lacking the small 2[4Fe-4S] cluster-containing FwdG subunit. While native electrophoresis indicates a major and minor species compatible with an FmdABCD₂F monomeric and dimeric oligomer, respectively, size exclusion chromatography rather indicates a dimeric organization (Figure S1B and C). We therefore suspect that the complex is disrupted during electrophoresis and concluded that a (FmdABCD₂F)₂ species is the principal component. The purified enzyme is catalytically active, performing the viologen-dependent reduction of CO₂ and oxidation of both formate and the MFR-analogue furfurylformamide (FFA, Table 1), with kinetic parameters similar to those previously published for homologous enzymes.^[16,17] Viologen-supported CO₂ reduction turnover measured in solution is around 400-fold lower than that measured with FDH in similar conditions.^[18] This was expected as i) in the absence of a

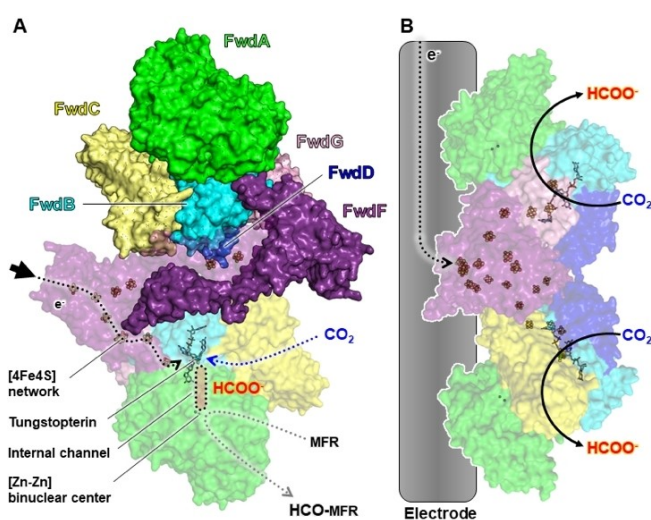


Figure 1. Structure and mechanism of formyl-MFR complex. A. Top view of the crystal structure of the Fwd dimer from the thermophilic archaeon *Methanothermobacter wolfeii* (PDB: 5T5M). The enzyme is coloured by subunit, with a monomer being represented as surface, and the other as transparent surface. A thick black arrow indicates the suspected entry point of electrons. Dashed lines highlight the different tunnels and cavity involved in reaction: electron transfer (black), hydrophobic CO₂ tunnel (blue), hydrophilic formate tunnel (red) and MFR binding site (grey). B. Bioelectrocatalytic CO₂ reduction by dimeric Fwd adsorbed to a graphite rod electrode (GRE). Cofactors are represented as balls and sticks with carbon, oxygen, nitrogen, sulphur, iron, phosphorus, tungsten and zinc atoms coloured in white, red, blue, yellow, orange, light orange, cyan and green, respectively. Despite the simplified depiction, a distribution of Fwd orientation on the electrode is expected.

Table 1: Kinetic parameters of the purified MsFmd in solution and in homologous systems. The K_{cat}^{app} was calculated based on a molecular weight of 198.50 kDa corresponding to the monomeric Fmd. All measurements were performed at least in triplicates.

Substrate	K_M^{app} (mM)	V_{max}^{app} (U.mg ⁻¹)	k_{cat}^{app}
MsFmd			
CO ₂	ND	0.24 ± 0.03*	0.794 s ⁻¹ *
Formate	183.39 ± 28.7	0.92 ± 0.07	3.044 s ⁻¹
Furfurylformamide	41.04 ± 12.1	6.58 ± 0.65	21.77 s ⁻¹
MbFmd^a			
Formate	1,700	1.8	6.60 s ⁻¹ b
Furfurylformamide	200	20	73.33 s ⁻¹ b
MwFmd^a			
Formate	35	1.2	2.60 s ⁻¹ b
Furfurylformamide	53	0.3	0.65 s ⁻¹ b

*The kinetics parameters of CO₂ reduction were determined with a saturating concentration of 100 mM NaHCO₃. [a] The values for the Mo-dependent complexes from *Methanosarcina barkeri* and *Methanothermobacter wolfeii* (MbFmd and FwFmd) as well as for the W-dependent enzyme from *M. wolfeii* (MwFwd) are derived from Bertram *et al.*, 1994.^[16] [b] The molecular weight used for calculation are derived from Wagner, Ermler and Shima (2018),^[13] and corresponds to a single monomer. ND: not-determined.

formyl-carrier, formate can accumulate within the enzyme and its low diffusion would retard CO_2 reduction; ii) the redox potential of the reaction performed by *MsFmd* (CO_2 /formyl-MFR couple, potential estimated to be $E^0 = -0.530 \text{ V}^{[13]}$) is considerably lower than that of FDH ($\text{CO}_2/\text{HCOO}^-$ couple, $E^0 = -0.420 \text{ V}^{[10,19]}$) and therefore the cofactors in *MsFmd* are expected to exhibit lower potentials than that of FDH, limiting electron transfer from methyl viologen ($E^0 = -0.446 \text{ V}^{[20]}$). The formate oxidation activity of *MsFmd* is also lower than that of FDHs, as the enzyme exhibits poor affinity for formate (Table 1). This is coherent with the proposed reaction mechanism of these enzymes, in which formate is an intermediate trapped in the internal cavity. This intrinsic property would be advantageous for electrochemical CO_2 reduction applications as formate oxidation rates would not compete with CO_2 reduction.

The *MsFmd* enzyme was immobilised on to the electrode by simple adsorption and no external redox mediator was included. Cyclic voltammograms (CV) measured before and after the addition of 100 mM NaHCO_3 as a source of CO_2 show a HCO_3^- -dependent reduction current, attributed to CO_2 reduction to formate under these working conditions, as no formyl carriers are available (Figure 2A). The data indicate an approximate onset potential of -0.45 V (vs. SHE), beyond which a significant negative (reductive)

current for substrate reduction is evident. A more positive onset potential would normally be expected for CO_2 reduction in the absence of formate in the bulk ($E^0 = -0.420 \text{ V}^{[19]}$). We hypothesize that this reflects the relatively negative E^0 values of FeS clusters of Fmd compared to those of FDHs. CV experiments carried out with 100 mM sodium formate instead of NaHCO_3 yielded unreproducible results, except if the protein adsorption promoter neomycin^[21] was included in the electrolyte (Figure S2). In the presence of neomycin, formate addition led to a weak oxidative activity, several fold lower than that measured with NaHCO_3 (Figure 2B). Furthermore, formate oxidation could not be monitored in the presence of both 100 mM NaHCO_3 and 100 mM formate (Figure 2C). The weak formate electrooxidation activity can be explained by the apparent low affinity of the enzyme for formate. The reasons for the apparent competition between CO_2 and formate might come from the access to the active site, which remains to be experimentally verified. No activity could be detected for both reactions using an oxygen-inactivated enzyme (Figure 2D).

Non-turnover redox peaks are present in the CVs of *MsFmd* in the absence of substrate, although here we refrain from directly assigning values of E^0 of the enzyme (where we assume $E^0 = E_m$) since (i) there are many FeS clusters present in *MsFmd* (which may undergo direct electron transfer with the electrode) and (ii) the reductant dithiothreitol (DTT) is present in the preparation of *MsFmd*. To address this, we performed an additional wash of *MsFmd* immediately prior to electrochemical analysis (Figure S3) to remove residual DTT. After washing, these redox peaks virtually disappear. We conclude that these redox peaks may have then been due to DTT present in the sample, or that the absence of DTT results in the rapid degradation of the complex (explaining the comparatively lower electrocatalytic currents that are observed after washing, (Figure S3)). We therefore sought to estimate the E^0/E_m of *MsFmd* using the catalytic response in the presence of NaHCO_3 . The potential at $i_{\text{cat}/2}$ was used to estimate the standard enzyme potential for catalysis ($E_{\text{cat}/2} = E^0_{\text{app}} \approx -0.510 \text{ V}$ vs. SHE, Figure S4). The calculated E^0_{app} value is similar to the estimated E^0 of the CO_2 /Formyl-MFR couple (-0.530 V vs. SHE).^[13,22]

The steady-state catalytic currents were measured to determine the kinetic parameters of GRE-bound *MsFmd* (Figure 3A–C, Table S1). The apparent Michaelis constant (K_M^{app}) and the apparent maximum current density ($J_{\text{max}}^{\text{app}}$) were determined by nonlinear regression to be $3.8 \pm 0.3 \text{ mM}$ CO_2 and $124 \pm 17 \mu\text{A cm}^{-2}$, respectively (Table 2). This current density is within the range obtained with FDHs (5 to $200 \mu\text{A cm}^{-2}$),^[6,23–25] showing that simple adsorption of *MsFmd* on GRE yields a potent electrochemical CO_2 reduction system. This is particularly impressive considering the difference in viologen-based CO_2 reduction rates measured in solution.

GRE-bound *MsFmd* exhibits an affinity for CO_2 on the same order of magnitude as that determined in the Fmd complex from *Methanosarcina barkeri* (0.7 mM)^[26] and FDHs (0.420 – 2.7 mM).^[18,19,25] However, a drastic difference

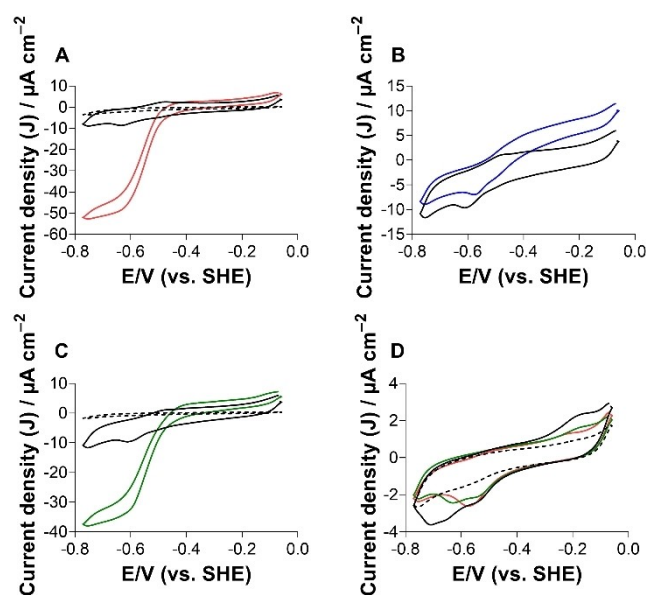


Figure 2. CVs of CO_2 reduction/formate oxidation catalysed by *MsFmd* on GRE. A. Representative CV of a *MsFmd*-bound GRE in the presence of 100 mM NaHCO_3 (red) in 0.1 M MOPS buffer (pH 7.0). B. Representative CV of *MsFmd*-bound GRE in the presence of 100 mM formate (blue) in 0.1 M MOPS buffer (pH 7.0) and 4 mM neomycin. C. Representative CV of a *MsFmd*-bound GRE in the presence of 100 mM NaHCO_3 and 100 mM formate (green) in 0.1 M MOPS buffer (pH 7.0) and 4 mM neomycin. D. Representative CV of an O_2 -inactivated *MsFmd*-bound GRE in the absence (black) and presence (red) of 100 mM NaHCO_3 and 100 mM formate (green). The recorded voltammograms with bare electrodes are shown as dashed traces; background cycles recorded in the absence of any substrate are also shown (black solid line). All experiments were performed by stirring at 22°C and a scan rate of 5 mV s^{-1} .

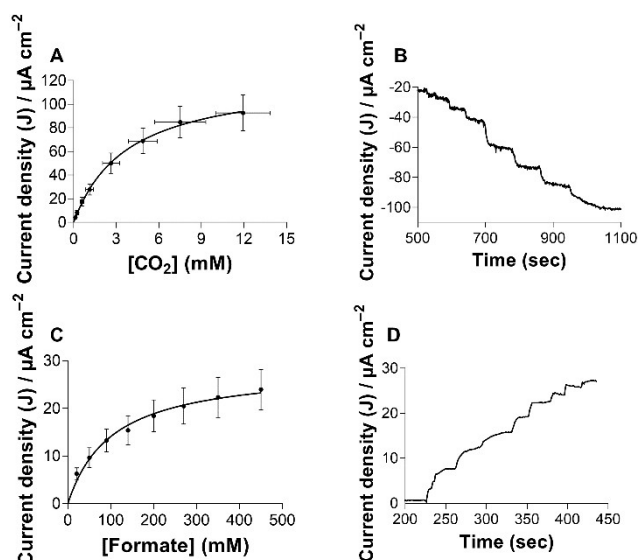


Figure 3. Steady-state kinetic study of MsFmd-bound GREs. Kinetic parameters of CO₂ reduction (A and B) and formate oxidation (C and D). A potential of -0.63 V vs. SHE was applied to the GREs for CO₂ reduction, whereas a potential of -0.2 V vs. SHE was applied to the GREs for formate oxidation. All experiments were performed in a stirred MOPS buffer solution (pH 7.0) at 50°C , and successive injections of either NaHCO₃ or formate were made. Current densities (j) are plotted as the current density magnitudes in the case of CO₂ reduction since a reductive reaction yields an increasingly negative current density. Panels B and D show representative i - t curves for the two electroenzymatic reactions (data used to plot the K_M fits). Standard error (SE) was calculated based on three replicates of each sample concentration.

Table 2: Kinetic parameters of MsFmd bound on electrode and calculated Faradaic efficiency for CO₂ reduction.

Kinetic parameters			
Substrate	K_M^{app} (mM)	$j_{\text{max}}^{\text{app}}$ ($\mu\text{A}\cdot\text{cm}^{-2}$)	
CO ₂	3.8 ± 1.3	124 ± 17	
Formate	103 ± 45	29 ± 4	
Faradaic efficiency			
Formate calculated (nmol)	Formate detected (nmol)	Charged passed (mC)	Formate efficiency (%)
375 ± 77	408 ± 79	723 ± 18	109 ± 1

Potentiostatic bulk electrolysis was performed for 180 min at -0.63 V vs. SHE in 0.1 M MOPS (pH 7.0) containing 100 mM NaHCO₃ at 50°C (balance Ar). All measurement were performed in triplicates.

exists for formate: in characterized FDHs,^[18,19,27] the affinity for formate is superior or in the range of that for CO₂, while Fmds/Fwds generally exhibit comparatively high K_M for formate as the molecule is not the substrate.^[16] Accordingly, the K_M^{app} for formate of GRE-bound MsFmd was calculated to be 103 ± 45 mM formate, similar to that estimated with the enzyme in solution, with a maximal current density estimated to be 29 ± 4 $\mu\text{A}\cdot\text{cm}^{-2}$ (Figure 3C–D and Table 2).

Enzymatic quantification of formate after bulk bioelectrocatalytic CO₂ reduction confirmed its production with high efficiency (109 ± 1 % of CO₂ converted into formate, Figure S5, Table 2). Hence, no significant amount of alternative product is synthesized in the electrode working conditions. This efficiency of over 100 % likely originates from the secondary enzymatic assay for resulting formate oxidation (detailed in the Supporting Information). While the activity decreases with time, possibly due to enzyme inactivation of the release of the electrode, it was nevertheless possible to monitor CO₂ reduction after 3 hours at 50°C (Figure S5).

Our study revealed for the first time how formyl-MFR dehydrogenase complexes from methanogens can be employed as biocatalysts for CO₂ reduction to formate when bound on graphite electrodes. Unlike characterised FDHs, the enzyme presents weak formate oxidation activity, which is disabled in the presence of CO₂, leading to formate accumulation during electrocatalysis. The efficiency of the system is in the same range as that obtained with FDHs considering current density and formate accumulation.^[6,23,24] The non-physiological generation of formate should be impaired by several structural features of the enzyme (Figure 1A), and bioengineering will be necessary to unleash its full formate-production potential. Modification of the CO₂-diffusion tunnel, the [Zn–Zn] binuclear formate condensation site, the MFR binding interface (or even complete removal of the FmdA subunit) could, in theory, considerably enhance the formate generation rates, as they are superfluous for CO₂ reduction applications. Before undertaking such modifications, more insights into the mechanism of Fmds are imperative, and future works must capture new states of the complex under turnover conditions to unveil how this impressive multi-enzymatic machine operates.

Supporting Information

The authors have cited additional references within the Supporting Information.^[18,22,28–32] Raw data are freely available on Zenodo (DOI: 10.5281/zenodo.8250713).

Acknowledgements

This project has received funding from the European Union's Horizon 2020 research and innovation program under the Marie Skłodowska-Curie grant agreement No 101024443. C.W. and J.M.K. were supported by the SIAM gravitation program (grant #024002002) granted by the Netherlands Organization for Scientific Research and the Ministry of Education, Culture and Science. J.M.K. was furthermore supported by the Deutsche Forschungs Gesellschafts (DFG) Grant KU 3768/1-1. O.L.N., M.B. and T.W. thank the Max Planck Institute for Marine Microbiology and the Max Planck Society for their continuous support, as well as Christina Probian and Ramona Appel for their continuous support in the Microbial Metabolism laboratory. S.S. and R.D.M. thank the staff of the University of Geneva's Department of Inorganic and Analytical

Chemistry for their support. Open Access funding provided by Université de Genève.

Conflict of Interest

The authors declare no conflict of interest.

Data Availability Statement

The data that support the findings of this study are openly available in Zenodo at <https://doi.org/10.5281/zenodo.8250713>, reference number 8250713.

Keywords: Bioelectrocatalysis · CO₂-Sequestration · Direct Electron Transfer · Formylmethanofuran Dehydrogenase · Molybdopterin Cofactor

- [1] M. Tiberti, E. Papaleo, N. Russo, L. De Gioia, G. Zampella, *Inorg. Chem.* **2012**, *51*, 8331–8339.
- [2] B. Yao, T. Xiao, O. A. Makgae, X. Jie, S. Gonzalez-Cortes, S. Guan, A. I. Kirkland, J. R. Dilworth, H. A. Al-Megren, S. M. Alshihri, P. J. Dobson, G. P. Owen, J. M. Thomas, P. P. Edwards, *Nat. Commun.* **2020**, *11*, article: 6395.
- [3] T. Liu, Q. Wang, G. Wang, X. Bao, *Green Chem.* **2021**, *23*, 1212–1219.
- [4] W. Liu, P. Zhai, A. Li, B. Wei, K. Si, Y. Wei, X. Wang, G. Zhu, Q. Chen, X. Gu, R. Zhang, W. Zhou, Y. Gong, *Nat. Commun.* **2022**, *13*, article: 1877.
- [5] D. L. Dubois, *Encyclopedia of Electrochemistry* (Ed.: A. J. Bard, M. Stratmann), Volume 7a: Inorganic Chemistry, VCH, Weinheim, **2006**, p. 202–225.
- [6] T. Reda, C. M. Plugge, N. J. Abram, J. Hirst, *Proc. Natl. Acad. Sci. USA* **2008**, *105*, 10654–10658.
- [7] K. Schuchmann, V. Müller, *Science* **2013**, *342*, 1382–1386.
- [8] A. Bar-Even, *Biochemistry* **2016**, *55*, 3851–3863.
- [9] S. Enthaler, *ChemSusChem* **2008**, *1*, 801–804.
- [10] O. N. Lemaire, M. Jespersen, T. Wagner, *Front. Microbiol.* **2020**, *11*, article: 486.
- [11] I. A. Berg, D. Kockelkorn, W. H. Ramos-Vera, R. F. Say, J. Zarzycki, M. Hügler, B. E. Alber, G. Fuchs, *Nat. Rev. Microbiol.* **2010**, *8*, 447–460.
- [12] W. F. Martin, R. K. Thauer, *Cell* **2017**, *168*, 953–955.
- [13] T. Wagner, U. Ermler, S. Shima, *Formylmethanofuran dehydrogenase, in Encyclopedia of inorganic and bioinorganic chemistry*, (Ed.: R. A. Scott), John Wiley & Sons, Ltd, Hoboken, **2018**, pp.1–18.
- [14] T. Watanabe, O. Pfeil-Gardiner, J. Kahnt, J. Koch, S. Shima, B. J. Murphy, *Science* **2021**, *373*, 1151–1156.
- [15] T. Wagner, U. Ermler, S. Shima, *Science* **2016**, *354*, 114–117.
- [16] P. A. Bertram, M. Karrasch, R. A. Schmitz, R. Bocher, S. P. Albracht, R. K. Thauer, *Eur. J. Biochem.* **1994**, *220*, 477–484.
- [17] R. K. T. J. Breitung, G. Börner, M. Karrasch, A. Berkessel, *FEBS Lett.* **1990**, *268*, 257–260.
- [18] A. R. Oliveira, C. Mota, C. Mourato, R. M. Domingos, M. F. A. Santos, D. Gesto, B. Guigliarelli, T. Santos-Silva, M. J. Romão, I. A. Cardoso Pereira, *ACS Catal.* **2020**, *10*, 3844–3856.
- [19] X. Yu, D. Nicks, A. Mulchandani, R. Hille, *J. Biol. Chem.* **2017**, *292*, 16872–16879.
- [20] L. Michaelis, E. S. Hill, *J. Gen. Physiol.* **1933**, *16*, 859–873.
- [21] Y. Sugimoto, Y. Kitazumi, S. Tsujimura, O. Shirai, M. Yamamoto, K. Kano, *Biosens. Bioelectron.* **2015**, *63*, 138–144.
- [22] P. A. Bertram, R. K. Thauer, *Eur. J. Biochem.* **1994**, *226*, 811–818.
- [23] A. Bassegoda, C. Madden, D. W. Wakerley, E. Reisner, J. Hirst, *J. Am. Chem. Soc.* **2014**, *136*, 15473–15476.
- [24] J. Alvarez-Malmagro, A. R. Oliveira, C. Gutiérrez-Sánchez, B. Villajos, I. A. C. Pereira, M. Vélez, M. Pita, A. L. De Lacey, *ACS Appl. Mater. Interfaces* **2021**, *13*, 11891–11900.
- [25] M. Yuan, S. Sahin, R. Cai, S. Abdellaoui, D. P. Hickey, S. D. Minter, R. D. Milton, *Angew. Chem. Int. Ed.* **2018**, *57*, 6582–6586.
- [26] J. A. Vorholt, R. K. Thauer, *Eur. J. Biochem.* **1997**, *248*, 919–924.
- [27] W. E. Robinson, A. Bassegoda, E. Reisner, J. Hirst, *J. Am. Chem. Soc.* **2017**, *139*, 9927–9936.
- [28] J. M. Kurth, M. C. Müller, C. U. Welte, T. Wagner, *Microorganisms* **2021**, *9*, 837.
- [29] O. N. Lemaire, P. Infossi, A. Ali Chaouche, L. Espinosa, S. Leimkühler, M. T. Giudici-Orticoni, V. Méjean, C. Iobbi-Nivol, *Sci. Rep.* **2018**, *8*, article: 13576.
- [30] A. M. Appel, M. L. Helm, *ACS Catal.* **2014**, *4*, 630–633.
- [31] A. Dinu, C. Apetrei, *Chemosensors* **2022**, *10*, 180.
- [32] V. Fourmond, C. Léger, I. Electrochemistry, *Curr. Opin. Electrochem.* **2017**, *1*, 110–120.

Manuscript received: August 16, 2023

Accepted manuscript online: September 15, 2023

Version of record online: September 29, 2023